Dual Detection-Guided Newborn Target Intensity Based on Probability Hypothesis Density for Multiple Target Tracking

Li Gao*, Yongjie Ma
Department of Mechanical and Electronic Engineering, Shangqiu Polytechnic
Shangqiu, 476000, China
[e-mail: sifsrp@163.com]
*Corresponding author: Li Gao

Received February 13, 2016; revised June 15, 2016; revised August 15, 2016; accepted August 8, 2016; published October 31, 2016

Abstract

The Probability Hypothesis Density (PHD) filter is a suboptimal approximation and tractable alternative to the multi-target Bayesian filter based on random finite sets. However, the PHD filter fails to track newborn targets when the target birth intensity is unknown prior to tracking. In this paper, a dual detection-guided newborn target intensity PHD algorithm is developed to solve the problem, where two schemes, namely, a newborn target intensity estimation scheme and improved measurement-driven scheme, are proposed. First, the newborn target intensity estimation scheme, consisting of the Dirichlet distribution with the negative exponent parameter and target velocity feature, is used to recursively estimate the target birth intensity. Then, an improved measurement-driven scheme is introduced to reduce the errors of the estimated number of targets and computational load. Simulation results demonstrate that the proposed algorithm can achieve good performance in terms of target states, target number and computational load when the newborn target intensity is not predefined in multi-target tracking systems.

Keywords: Multi-target tracking, probability hypothesis density, newborn target intensity, Gaussian mixture

This paper is supported by the key scientific research project of Henan higher education institution (No. 16A520066 and 17A520052).

http://dx.doi.org/10.3837/tiis.2016.10.025 **ISSN : 1976-7277**

1. Introduction

In recent years, multi-target tracking based on the random finite sets (RFS) theory [1] as an alternative to the classical data association-based target tracking algorithm has attracted considerable attention. Three suboptimal approximations, namely, the Probability Hypothesis Density (PHD) [2], Cardinalized PHD (CPHD) [3], and Multi-Bernoulli (MeMBer) [4] were developed as alternative methods to the RFS-based Bayesian multi-target tracking. The Sequence Monte Carlo PHD (SMC-PHD) [5] and Gaussian Mixture PHD (GM-PHD) [6] are two closed-form solutions to the PHD filter. The two implementations of the PHD filter and its modified versions [7]-[9] were widely applied to multi-target tracking [10]-[12]. More recently, the concept of the labeled RFS and its implementations, named Labeled Multi-Bernoulli [13] and Generalized Labeled Multi-Bernoulli (GLMB) [14][15], were introduced to cope with multi-target tracking.

According to the framework of the PHD filter, there is a fundamental assumption that the newborn target intensity is known as a priori. However, the assumption is not applicable to real multi-target tracking problems because birth targets may randomly appear at any time and position in real environments. A number of PHD-based multi-target tracking algorithms were developed to solve this problem. Ristic et al. [16] proposed an adaptive target birth intensity PHD filter using a Sequence Monte Carlo implementation, where the unknown target birth intensity is estimated using all current measurements and a measurement likelihood function. However, the adaptive target birth intensity PHD filter has a disadvantage that the estimated number of targets may have relatively larger deviations in dense clutter environments. Moreover, birth targets can appear anywhere in the entire surveillance region, which makes the computational burden of the adaptive target birth intensity PHD filter relatively high. Wang et al. [17] developed an improved multi-target Bayesian filter based on a target track initiation scheme that uses the sequential probability ratio test to detect birth targets. Due to the fact that some measurements may be forbidden to initialize target tracks, the proposed approach fails to track birth targets in closely spaced target scenarios. Zhang et al. [18] proposed an improved GM-PHD filter based on the revised Gaussian component fusion scheme where each received measurement is associated with one Gaussian component. Although the proposed algorithm can obtain better target birth intensity estimates, it suffers from heavy computational load which is nearly double that of the GM-PHD filter. Zhou et al. [19] proposed a target birth intensity estimation algorithm for tracking visual targets, where the entropy distribution and coverage rate are introduced to model the newborn target intensity. However, the entropy distribution and coverage rate-based newborn target estimation scheme is only suitable to computer vision because the estimates of birth targets rely on both the intersection rate and area rate of different birth targets. Recently, Zhu et al. [20] developed an extended GM-PHD filter, where a new estimation scheme combining with the single-point and two-point difference track initialization methods is proposed. Compared with the adaptive target birth intensity PHD filter [16], the extended GM-PHD filter achieves better performances in different clutter rate and detection probability scenarios.

Inspired by the ideas of the detection-guided [17][21] and entropy distribution [19][22] methods, we propose a dual detection-guided newborn target intensity algorithm based on the PHD filter to track multiple targets. First, the newborn target intensity can be accurately estimated using the Dirichlet distribution and target velocity feature methods. Specifically, the Dirichlet distribution with negative exponent parameters is used to model the prior distribution

of the target birth intensity, where the possible newborn target intensity can be computed using the maximum a posteriori method. The latest obtained birth intensity is refined using the target velocity feature-based method, and an accurate estimation of the target birth intensity is ultimately achieved. To reduce the errors of the estimated number of targets in dense clutter scenarios and the computational load of the adaptive target birth intensity PHD filter, an improved measurement-driven scheme is proposed. Simulation results demonstrate that the proposed algorithm achieves better performance in terms of the OSPA distance and NTE compared with the adaptive target birth intensity PHD filter, and also leads to lower computational burden.

The remainder of this paper is structured as follows. Section 2 provides a brief overview of random finite sets, the PHD filter, and Gaussian mixture PHD. The newborn target intensity estimation and improved measurement-driven schemes along with the steps of the proposed algorithm are detailed in Section 3. In Section 4, the performance comparison of different algorithms is presented in several tracking scenarios. Finally, the conclusions are given in Section 5.

2. Background

2.1 Random finite sets and the PHD Filter

In the RFS theoretical framework, the respective collections of target states and observations at time k are represented as finite sets $X_k = \{x_{k,1},...,x_{k,N_k}\}$ and $Z_k = \{z_{k,1},...,z_{k,M_k}\}$, where N_k and M_k are the cardinalities of the target set X_k and observation set Z_k, respectively.

The PHD filter propagates the first-order statistical moment of the RFS of target states using the PHD recursion, which consists of the prediction and update steps. Let $D_{k-1}(x \mid Z^{(k-1)})$ denote the multi-target posterior intensity at time $k-1$. The prediction equation of the PHD filter is given by

$$D_{k|k-1}(x \mid Z^{(k-1)}) = \int \left[p_{S,k}(\zeta) f_{k|k-1}(x \mid \zeta) + \beta_{k|k-1}(x \mid \zeta) \right] D_{k-1}(\zeta \mid Z^{(k-1)}) d\zeta + \gamma_k(x) \quad (1)$$

where x is the target state, $Z^{(k-1)} = \{Z_1,...,Z_{k-1}\}$ is the union of the measurement sets up to time $k-1$, $p_{S,k}(\zeta)$ is the survival probability that a target still exists at time k given that its previous state is ζ, $f_{k|k-1}(x \mid \zeta)$ is the transition probability of target state, $\gamma_k(x)$ is the newborn target intensity, and $\beta_{k|k-1}(x \mid \zeta)$ is the intensity of the $\beta_{k|k-1}(\zeta)$ spawned at time k by a target with previous state ζ.

When the measurement set Z_k is available at time k, the update equation of the PHD filter can be computed as

$$D_k(x \mid Z^{(k)}) = \left[1 - p_{D,k}(x)\right] D_{k|k-1}(x \mid Z^{(k-1)}) + \sum_{z \in Z_k} \frac{p_{D,k}(x) g_k(z \mid x) D_{k|k-1}(x \mid Z^{(k-1)})}{\kappa_k(z) + \int p_{D,k}(x) g_k(z \mid x) D_{k|k-1}(x \mid Z^{(k-1)}) dx} \quad (2)$$

where $p_{D,k}(x)$ is the detection probability given a state x, and $g_k(z \mid x)$ is the single target likelihood. The intensity of the clutter RFS is represented by $\kappa_k(z) = \lambda_c C_k(z)$, where λ_c and $C_k(z)$ are the mean and probability density distribution of clutter, respectively.

2.2. Gaussian Mixture PHD Filter

For the linear Gaussian multi-target model, the Gaussian mixture PHD filter represents a closed-form solution of the PHD recursion as a weighted sum of Gaussian components.

Let $\mathcal{N}(\cdot;m,P)$ denote the Gaussian density with mean m and covariance P. Assume that each target follows a linear Gaussian dynamic model and the sensor has a linear Gaussian measurement model, namely,

$$f_{k|k-1}(x\,|\,\xi)=\mathcal{N}(x;F_{k-1}\xi,Q_{k-1}) \tag{3}$$

$$g_{k|k-1}(z\,|\,x)=\mathcal{N}(x;H_k x,R_k) \tag{4}$$

where F_{k-1} is the state transition matrix, Q_{k-1} is the process noise covariance, H_k is the measurement matrix, and R_k is the measurement noise covariance.

Assume that the posterior intensity at time $k-1$ is expressed as the following Gaussian mixture with J_{k-1} components:

$$v_{k-1}(x)=\sum_{i=1}^{J_{k-1}} w_{k-1}^{i}\,\mathcal{N}(x;m_{k-1}^{i},P_{k-1}^{i}) \tag{5}$$

Then, the predicted intensity at time k is also a Gaussian mixture with $J_{k|k-1}$ components and is given by

$$v_{k|k-1}(x)=\sum_{i=1}^{J_{k|k-1}} w_{k|k-1}^{i}\,\mathcal{N}(x;m_{k|k-1}^{i},P_{k|k-1}^{i}) \tag{6}$$

Based on the latest measurement set Z_k, the posterior intensity at time k is a Gaussian mixture given by

$$v_k(x)=(1-p_{D,k})v_{k|k-1}(x)+\sum_{z\in Z_k}\sum_{i=1}^{J_{k|k-1}} w_k^{i}(z)\,\mathcal{N}(x;m_{k|k}^{i},P_{k|k}^{i}) \tag{7}$$

where w_k^i is the weight of the ith target having the form

$$w_k^{i}(z)=\frac{p_{D,k}w_{k|k-1}^{i}\,g(z\,|\,x^{i})}{\kappa_k(z)+p_{D,k}\sum_{j=1}^{J_{k|k-1}} w_{k|k-1}^{j}\,g(z\,|\,x^{j})} \tag{8}$$

For simplicity, the main architecture of the GM-PHD filter is briefly summarized as above. The detailed process of the GM-PHD filter can be found in [6].

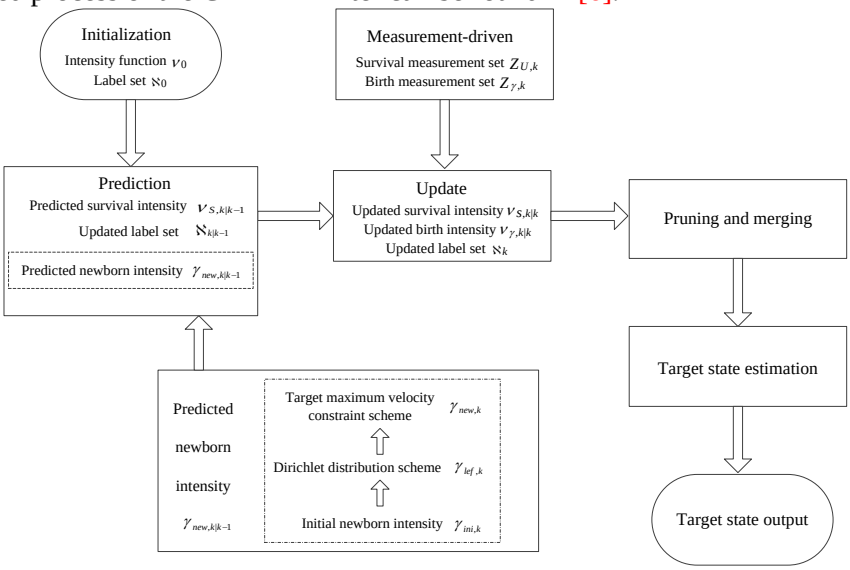

Fig. 1. Flow chart of the proposed algorithm

3. Dual Detection-Guided Newborn Target Intensity PHD Algorithm

In this section, a dual detection-guided newborn target intensity PHD algorithm is proposed. First, a newborn target intensity estimation scheme based on the Dirichlet distribution [23] and target velocity feature methods is designed to estimate the target birth intensity. Then, the improved measurement-driven scheme is incorporated into the adaptive target birth intensity PHD filter to reduce the interference of irrelevant measurements in the update step. The flow chart of the proposed algorithm is shown in **Fig. 1**.

3.1 Newborn Target Intensity Initialization

Each target is assigned a unique label ℓ to distinguish from others, where the Gaussian components of each target have the same label. At time $k-1$, the target state estimate set $\vartheta_{E,k-1}$ and corresponding label set $\aleph_{E,k-1}$ can be computed as

$$\vartheta_{E,k-1}=\left\{m_{k-1}^{i}: w_{k-1}^{i}>w_{th},\ i=1,\ldots J_{k-1}\right\} \tag{9}$$

$$\aleph_{E,k-1}=\left\{\ell_{k-1}^{i}: w_{k-1}^{i}>w_{th},\ i=1,\ldots J_{k-1}\right\} \tag{10}$$

where J_{k-1} is the number of Gaussian components, and w_{th} is the target state estimate threshold.

Based on the latest measurement set $Z_k=\left\{z_k^j\right\}_{j=1}^{M_k}$ at time k, the measurement set $Z_{E,k}$ associated with the set $\vartheta_{E,k-1}$ is given by

$$Z_{E,k}=\left\{z_k^j: \arg\min_j\left(\left(z_k^j-H_k m_{E,k|k-1}^{i}\right)^T\left(S_{E,k}^{i}\right)^{-1}\left(z_k^j-H_k m_{E,k|k-1}^{i}\right)\right)\right\},\quad z_k^j\in Z_k,\forall j=1:M_k \tag{11}$$

$$m_{E,k|k-1}^{i}=F_{k-1}m_{E,k-1}^{i} \tag{12}$$

$$S_{E,k}^{i}=H_k P_{E,k|k-1}^{i}H_k^T+R_k \tag{13}$$

$$P_{E,k|k-1}^{i}=Q_{k-1}+F_{k-1}P_{E,k-1}^{i}F_{k-1}^T \tag{14}$$

$$M_{E,k}=\rho\left(Z_{E,k}\right) \tag{15}$$

where $\rho(x)$ is a function that can compute the cardinality of a set.

After extracting $\vartheta_{E,k-1}$-associated measurements from Z_k, the residual measurement set $Z_{R,k}$ consisting of the most likely newborn target measurements and clutter and its cardinality $M_{R,k}$ are given by

$$Z_{R,k}=Z_k-Z_{E,k} \tag{16}$$

$$M_{R,k}=\rho\left(Z_{R,k}\right) \tag{17}$$

Due to the fact that newborn targets may randomly appear at any position in a real tracking environment, each measurement in $Z_{R,k}$ maybe a newborn target. Therefore, all measurements in $Z_{R,k}$ are used to model the initialized newborn target intensity $\gamma_{ini,k}$ given by

$$\gamma_{ini,k}=\sum_{i=1}^{M_{R,k}}w_{\gamma,k}^{i}\mathcal{N}\left(x;m_{\gamma,k}^{i},P_{\gamma,k}^{i}\right) \tag{18}$$

$$w_{\gamma,k}^{i}=1/M_{R,k};\ m_{\gamma,k}^{i}=H_k^{-1}z_k^{i};\ P_{\gamma,k}^{i}=H_k^{-1}R_k\left(H_k^{-1}\right)^T \tag{19}$$

To distinguish newborn targets, a unique label is assigned to each newborn target, where the newborn target label set is given by

$$\aleph_{\gamma,k}=\left\{\ell_{\gamma,k}^{1},\ldots,\ell_{\gamma,k}^{i},\ldots,\ell_{\gamma,k}^{M_{R,k}}\right\},\quad \forall i=1:M_{R,k} \tag{20}$$

3.2 Dirichlet Distribution-Based Newborn Target Intensity Update

Assume that the mean and covariance of the *ith* Gaussian component in $\gamma_{ini,k}$ is represented by the set $\alpha_i = \{m^i_{\gamma,k}, P^i_{\gamma,k}\}$. All the $M_{R,k}$ Gaussian components can be given by $\alpha = \{w^i_{\gamma,k}, \ldots, w^{M_{R,k}}_{\gamma,k}, \alpha_i, \ldots, \alpha_{M_{R,k}}\}$. Due to measurement-originated uncertainty, the clutter in $Z_{R,k}$ are previously used to model $\gamma_{ini,k}$. To refine $\gamma_{ini,k}$, the Dirichlet distribution with negative exponent parameters is utilized to model the prior of the set α as follows:

$$p(\alpha) = \exp\left(\sum_{i=1}^{M_{R,k}} (-N/2) \log w^i_{\gamma,k}\right) \tag{21}$$

where N is the number of the elements of each component [24]. Clearly, the prior distribution of α relies on the weights of the Gaussian components. To remove the clutter-related components from $\gamma_{ini,k}$, the maximum a posteriori method is introduced to update the set α using the measurement set $Z_{k+1} = \{z^j_{k+1}\}_{j=1}^{M_{k+1}}$ at time $k+1$. In each iteration of the maximum a posteriori method, clutter-related components are deleted by changing their weights.

Assume that at time $k+1$, the log-likelihood of the set Z_{k+1} is

$$\log p(Z_{k+1} | \alpha) = \sum_{j=1}^{M_{k+1}} \log \sum_{i=1}^{M_{R,k}} w^i_{\gamma,k} g(z^j_{k+1} | \alpha_i) \tag{22}$$

where $g(z^j_{k+1} | \alpha_i)$ is the single-target likelihood. Using the maximum a posteriori method, the set α can be estimated as

$$\tilde{\alpha} = \arg\max_{\alpha} \{\log p(Z_{k+1} | \alpha) + \log p(\alpha)\} \tag{23}$$

Based on the weights of the Gaussian components in Eq.19, the sum of the weights of the newborn target components is

$$\sum_{i=1}^{M_{R,k}} w^i_{\gamma,k} = 1 \tag{24}$$

To estimate the weight $w^i_{\gamma,k}$ of the *ith* component, the partial derivative of the log-likelihood with respect to the weight $w^i_{\gamma,k}$ is set to zero under the constraint from Eq. 24

$$\frac{\partial}{\partial w^i_{\gamma,k}} \left(\log p(Z_{k+1} | \alpha) + \log p(\alpha) + \lambda \left(\sum_{i=1}^{M_{R,k}} w^i_{\gamma,k} - 1 \right) \right) = 0 \tag{25}$$

where λ is the Lagrange multiplier. The maximum a posteriori estimation of the weight $w^i_{\gamma,k}$ can be computed using the Lagrange multiplier method.

$$w^i_{\gamma,k} = \frac{\sum_{j=1}^{M_{k+1}} \xi_i(z^j_{k+1}) - N/2}{M_{k+1} - M_{R,k} N/2} \tag{26}$$

$$\xi_i(z^j_{k+1}) = \frac{w^i_{\gamma,k} g(z^j_{k+1} | \alpha_i)}{\sum_{i=1}^{M_{R,k}} w^i_{\gamma,k} g(z^j_{k+1} | \alpha_i)} \tag{27}$$

Similarly, the maximum a posteriori estimation of the mean $m^i_{\gamma,k}$ and covariance $P^i_{\gamma,k}$ are given by

$$m^i_{\gamma,k} = \mu^{-1} \sum_{j=1}^{M_{k+1}} \xi_i(z^j_{k+1}) H_k^{-1} z^j_{k+1} \tag{28}$$

$$P^i_{\gamma,k} = \mu^{-1} \sum_{j=1}^{M_{k+1}} \xi_i(z^j_{k+1}) (H_k^{-1} z^j_{k+1} - m^i_{\gamma,k})(H_k^{-1} z^j_{k+1} - m^i_{\gamma,k})^T \tag{29}$$

$$\mu = \sum_{j=1}^{M_{k+1}} \xi_i(z^j_{k+1}) \tag{30}$$

After each iteration, the *ith* component is removed from the set α if the weight $w_{\gamma,k}^{i}$ is below the threshold η_w. The weights of the remaining components are normalized for the next iteration. When the comparative difference rate of the log-posterior is less than the given threshold η_{dl}, the iteration terminates and the refined target birth intensity $\gamma_{lef,k}$ is obtained.

3.3 Target Velocity-Based Newborn Target Intensity Update

The Dirichlet distribution based newborn target intensity update method cannot completely remove clutter from $\gamma_{ini,k}$; that is, some clutter still exists in the refined birth intensity $\gamma_{lef,k}$. To accurately estimate the target birth intensity, the target velocity-based method is introduced to remove remaining clutter.

Assume that the state vector $x_k = \left[e_{x,k}, e_{y,k}, \tilde{e}_{x,k}, \tilde{e}_{y,k}\right]^T$ of each target consists of the position $\left[e_{x,k}, e_{y,k}\right]^T$ and velocity $\left[\tilde{e}_{x,k}, \tilde{e}_{y,k}\right]^T$ at time k. Then, the x-axis direction predicted velocity $\tilde{e}_{x,k|k-1}^{i}$ and y-axis direction predicted velocity $\tilde{e}_{y,k|k-1}^{i}$ of the *ith* target are given by

$$\tilde{e}_{x,k|k-1}^{i} = e_{x,k|k-1}^{i} - e_{x,k-1}^{i} \tag{31}$$

$$\tilde{e}_{y,k|k-1}^{i} = e_{y,k|k-1}^{i} - e_{y,k-1}^{i} \tag{32}$$

The respective maximum velocities of the *ith* target in the x- and y-axis direction up to time k are given by

$$\tilde{e}_{x,\max}^{i} = \arg\max\left(\left\{abs\left(\tilde{e}_{x,1}^{i}\right),...,abs\left(\tilde{e}_{x,j}^{i}\right),abs\left(\tilde{e}_{x,k|k-1}^{i}\right)\right\}\right),\ \ \forall j = 1:k-1 \tag{33}$$

$$\tilde{e}_{y,\max}^{i} = \arg\max\left(\left\{abs\left(\tilde{e}_{y,1}^{i}\right),...,abs\left(\tilde{e}_{y,j}^{i}\right),abs\left(\tilde{e}_{y,k|k-1}^{i}\right)\right\}\right),\ \ \forall j = 1:k-1 \tag{34}$$

where $abs(x)$ is the absolute value function. Under the assumption that the maximum velocities of targets in the current tracking scenario are close, the respective maximum velocities of all targets in the x- and y-axis direction up to time k can be given by

$$\tilde{e}_{x,\max} = \arg\max\left(\left\{\tilde{e}_{x,\max}^{1},...,\tilde{e}_{x,\max}^{i},...,\tilde{e}_{x,\max}^{L}\right\}\right),\ \ \forall i = 1:L \tag{35}$$

$$\tilde{e}_{y,\max} = \arg\max\left(\left\{\tilde{e}_{y,\max}^{1},...,\tilde{e}_{y,\max}^{i},...,\tilde{e}_{y,\max}^{L}\right\}\right),\ \ \forall i = 1:L \tag{36}$$

where L is the number of targets. Using the x-axis maximum velocity $\tilde{e}_{x,\max}$ and y-axis maximum velocity $\tilde{e}_{y,\max}$, the birth intensity $\gamma_{lef,k}$ can be further refined using the measurement set Z_{k+1}, and the comparatively accurate target birth intensity $\gamma_{new,k}$, along with the cardinality $M_{new,k}$ and label set $\aleph_{new,k}$, as follows

$$\gamma_{new,k} = \sum_{i=1}^{M_{new,k}} w_{\gamma,k}^{i} \mathcal{N}\left(x; m_{\gamma,k}^{i}, P_{\gamma,k}^{i}\right), \ell_k^i \in \aleph_{new,k}, \gamma_{new,k} \in \gamma_{lef,k} \tag{37}$$

$$M_{new,k} = \rho(\aleph_{new,k}) \tag{38}$$

$$\aleph_{new,k} = \left\{\ell_{\gamma,k}^{i} \mid req^{i} \triangleq true,\ \ \ell_{\gamma,k}^{i} \in \aleph_{lef,k}, \forall i = 1:M_{lef,k}\right\} \tag{39}$$

$$req^{i} = \begin{cases} true\ , & \begin{array}{c}\left(\tilde{e}_{x,\max} - 3\sigma_{\varepsilon} \le abs\left(\tilde{e}_{x,tem}^{i,j}\right) \le \tilde{e}_{x,\max} + 3\sigma_{\varepsilon}\right)\ and \\ \left(\tilde{e}_{y,\max} - 3\sigma_{\varepsilon} \le abs\left(\tilde{e}_{y,tem}^{i,j}\right) \le \tilde{e}_{y,\max} + 3\sigma_{\varepsilon}\right)\end{array} \\ false\ , & otherwise \end{cases} \tag{40}$$

$$\tilde{e}_{x,tem}^{i,j} = A\ H_k m_k^i - B\ z_{k+1}^j;\ \tilde{e}_{y,tem}^{i,j} = C\ H_k m_k^i - D\ z_{k+1}^j,\ z_{k+1}^j \in Z_{k+1}, \forall j = 1:M_{k+1} \tag{41}$$

where σ_{ε} is the standard deviation of the measurement noise, $M_{lef,k}$ is the number of the

Gaussian components of the intensity $\gamma_{lef,k}$, $\aleph_{lef,k}$ is the label set of the intensity $\gamma_{lef,k}$, and $\|x\|$ is the Euclid distance function. Further, A, B, C and D are four matrices, which are set to $A=[1,0,0,0]$, $B=[1,0]$, $C=[0,1,0,0]$ and $D=[0,1]$.

3.4 Improved ABI-GM-PHD algorithm

Owning to the advantages of the Gaussian mixture PHD filter in extracting target states, the adaptive target birth intensity PHD filter [16] is implemented using the framework of Gaussian mixture, denoted as the ABI-GM-PHD filter in this paper. The ABI-GM-PHD filter updates all targets using each measurement in Z_k at time k; therefore, the performance of the ABI-GM-PHD filter is not only affected by clutter, but also interfered by the measurements originated from survival targets and birth targets. In this section, an improved measurement -driven scheme for the ABI-GM-PHD filter is proposed to reduce disturbance from measurements in the update step.

(1) Measurements' Classification

According to predicted target states and the newborn target intensity, at each time step, measurements are classified as survival measurements, birth measurements, and clutter. Assume that the multi-target predicted intensity at time k can be approximated by

$$v_{k|k-1}(x)=p_{S,k}\sum_{i=1}^{J_{k|k-1}}w_{k-1}^{i}\mathcal{N}\left(x;m_{S,k|k-1}^{i},P_{S,k|k-1}^{i}\right)+\sum_{j=1}^{J_{\gamma,k}}w_{\gamma,k}^{j}\mathcal{N}\left(x;m_{\gamma,k}^{j},P_{\gamma,k}^{j}\right) \tag{42}$$

Eq.42 means that there are $J_{k|k-1}$ survival target components and $J_{\gamma,k}$ birth target components at time k. Therefore, a possible measurement associated with the *ith* survival target component, can be described as follows:

$$\tilde{z}_k^i=\left(z_k^n:\arg\min_n\left(z_k^n-m_{S,k|k}^i\right)^T\left(S_{S,k}^i\right)^{-1}\left(z_k^n-m_{S,k|k}^i\right)\right) \tag{43}$$

$$m_{S,k|k}^i=H_k m_{S,k|k-1}^i \tag{44}$$

$$S_{S,k}^i=H_k P_{S,k|k-1}^i H_k^T+R_k \tag{45}$$

where z_k^n denotes the *nth* measurement in the measurement set Z_k, and $S_{S,k}$ is the measurement residual covariance matrix. Accordingly, the survival measurement set $Z_{S,k}$ is formed as the union of associated measurements of $J_{k|k-1}$ survival target components, which can be approximated as

$$Z_{S,k}=\bigcup_{i=1}^{J_{k|k-1}}\tilde{z}_k^i \tag{46}$$

After extracting survival measurements, the residual measurements in Z_k are originated from spontaneous birth targets and clutter, which constitute the residual measurement set $Z_{b,k}$ as

$$Z_{b,k}=Z_k-Z_{S,k} \tag{47}$$

For $J_{\gamma,k}$ newborn target components, the associated birth measurement set $Z_{\gamma,k}$ can be obtained as follows:

$$D_{b,k}(z)=\left\{d_{\gamma,k}^{(1)}(z),...,d_{\gamma,k}^{(j)}(z)\mid z\in Z_{b,k},\forall j=1:J_{\gamma,k}\right\} \tag{48}$$

$$d_{\gamma,k}^{(j)}(z)=\left(z-H_k m_{\gamma,k}^j\right)^T\left(H_k P_{\gamma,k}^j H_k^T+R_k\right)^{-1}\left(z-H_k m_{\gamma,k}^j\right) \tag{49}$$

$$Z_{\gamma,k}=\left\{z_{\gamma,k}\mid D_{b,k}(z)\le\beta,z_{\gamma,k}\in Z_{b,k}\right\} \tag{50}$$

$$\beta=-2\ln(1-P_G)\quad for\ n_z=2 \tag{51}$$

where β is the gating threshold, and P_G is the probability of the target-originated measurements in the elliptical region. The dimension of the measurement is denoted by n_z.

(2) Main Steps of the Improved ABI-GM-PHD Algorithm

After extracting survival target measurements and birth target measurements, the remainder measurements in Z_k are considered as clutter. In order to achieve accurate estimates and lighter computational burden of the PHD filter, clutter is prohibited from updating targets. Based on the measurement sets $Z_{S,k}$ and $Z_{\gamma,k}$, the main steps of the improved ABI-GM-PHD algorithm are summarized as follows.

Prediction: Suppose that at time $k-1$, the survival target intensity can be approximated by

$$v_{S,k-1}(x)=\sum_{i=1}^{J_{S,k-1}} w_{S,k-1}^{i}\mathcal{N}\left(x;m_{S,k-1}^{i},P_{S,k-1}^{i}\right) \tag{52}$$

Further suppose that at time k the newborn target intensity can be obtained by Eq.37. Then, the multi-target predicted intensity $v_{k|k-1}$ is composed of the survival target predicted intensity $v_{S,k|k-1}$ and newborn target predicted intensity $\gamma_{new,k|k-1}$ as follows:

$$v_{k|k-1}=v_{S,k|k-1}+\gamma_{new,k|k-1} \tag{53}$$

$$v_{S,k|k-1}=\sum_{i=1}^{J_{S,k|k-1}} w_{S,k|k-1}^{i}\mathcal{N}\left(x;m_{S,k|k-1}^{i},P_{S,k|k-1}^{i}\right) \tag{54}$$

$$\gamma_{new,k|k-1}=\sum_{j=1}^{M_{new,k}} w_{\gamma,k|k-1}^{j}\mathcal{N}\left(x;m_{\gamma,k|k-1}^{j},P_{\gamma,k|k-1}^{j}\right) \tag{55}$$

$$w_{S,k|k-1}^{i}=p_{S,k}w_{S,k-1}^{i} \tag{56}$$

$$m_{S,k|k-1}^{i}=F_{k-1}m_{S,k-1}^{i} \tag{57}$$

$$P_{S,k|k-1}^{i}=Q_{k-1}+F_{k-1}P_{S,k-1}^{i}F_{k-1}^{T} \tag{58}$$

$$w_{\gamma,k|k-1}^{j}=w_{\gamma,k}^{j} \tag{59}$$

$$m_{\gamma,k|k-1}^{j}=m_{\gamma,k}^{j} \tag{60}$$

$$P_{\gamma,k|k-1}^{j}=P_{\gamma,k}^{j} \tag{61}$$

Update: Suppose that at time k the multi-target predicted intensity is given, approximated as in Eq.53. Then, the multi-target posterior intensity $v_{k|k}(x)$ can be computed as follows:

$$v_{k|k}(x)=v_{S,k|k}(x)+v_{\gamma,k|k}(x) \tag{62}$$

where the survival target posterior intensity $v_{S,k|k}(x)$ is given by

$$v_{S,k|k}(x)=\left(1-p_{D,k}\right)v_{S,k|k-1}(x)+\sum_{z\in Z_{S,k}}\sum_{i=1}^{J_{S,k|k-1}} w_{S,k|k}^{i}\mathcal{N}\left(x;m_{S,k|k}^{i},P_{S,k|k}^{i}\right) \tag{63}$$

$$w_{S,k|k}^{i}(z)=\frac{p_{D,k}w_{S,k|k-1}^{i}\mathcal{N}\left(z;\mu_{S,k|k-1}^{i},\eta_{S,k|k-1}^{i}\right)}{\Lambda(z)} \tag{64}$$

$$\Lambda(z)=\kappa_k(z)+\sum_{j=1}^{M_{new,k}} w_{\gamma,k}^{j}+\sum_{i=1}^{J_{S,k|k-1}} p_{D,k}w_{S,k|k-1}^{i}\mathcal{N}\left(z;\mu_{S,k|k-1}^{i},\eta_{S,k|k-1}^{i}\right) \tag{65}$$

$$\mu_{S,k|k-1}^{i}=H_k m_{S,k|k-1}^{i} \tag{66}$$

$$P_{S,k|k}^{i}=\left[I-K_k^{i}H_k\right]P_{S,k|k-1}^{i} \tag{67}$$

$$K_k^{i}=P_{S,k|k-1}^{i}H_k^{T}\left(\eta_{S,k|k-1}^{i}\right)^{-1} \tag{68}$$

$$\eta_{S,k|k-1}^{i}=H_k P_{S,k|k-1}^{i}H_k^{T}+R_k \tag{69}$$

The newborn target posterior intensity can be obtained by

$$v_{\gamma,k|k}(x)=\sum_{j=1}^{Z_{\gamma,k}} w_{\gamma,k|k}^{j}\mathcal{N}\left(x;m_{\gamma,k|k}^{j},P_{\gamma,k|k}^{j}\right) \tag{70}$$

$$w_{\gamma,k|k}^{j}=\frac{w_{\gamma,k|k-1}^{j}}{\Lambda(z)} \tag{71}$$

A pruning and merging mechanism is needed to keep the number of Gaussian components at a computationally tractable level. For the sake of simplicity, the detail step is omitted in this paper, which can be found in [6].

Remark 1. In the proposed algorithm, the survival target posterior intensity $v_{S,k|k}(x)$ (Eq.63) and newborn target posterior intensity $v_{\gamma,k|k}(x)$ (Eq.70) are approximated using the survival target measurement set $Z_{S,k}$ and birth target measurement set $Z_{\gamma,k}$, respectively. However, the ABI-GM-PHD filter computes the two posterior intensities of survival targets and newborn targets just using the measurement set Z_k, which is composed of survival target measurement set $Z_{S,k}$, newborn target measurement set $Z_{\gamma,k}$ and clutter. The objective of measurements' classification in Section 3.1 is to initialize newborn target intensity which will be used in the prediction step of the GM-PHD filter. The measurement sets $Z_{S,k}$ and $Z_{\gamma,k}$ obtained by the measurements' classification in Section 3.4 are used to update the targets in the update step of the GM-PHD filter.

4. Simulation Results

4.1 Experimental Parameters Setting

In this section, the effectiveness of the proposed approach is validated using the comparison of the ABI-GM-PHD filter, extended GM-PHD filter and proposed algorithm in several multi-target tracking experiments in the two-dimensional scene. The sample interval T is set to $T=1\text{s}$. Each target follows the dynamic model of Eq.3, and the measurement model is the same as in Eq.4, where the process noise covariance matrix $Q=diag([0.4,0.4])$, and the measurement noise matrix $R=diag([225,225])$. The running time comparison of the three algorithms is implemented on Dell computer with Inter(R) Core(TM) i5, 3.2GHz and 4GB RAM.

The respective probabilities of detection and survival are set to $p_{D,k}=0.99$ and $p_{S,k}=0.99$. P_G is 0.999 for both survival and newborn targets. The thresholds η_w and η_{dl} are empirically set to $\eta_w=10^{-3}$ and $\eta_{dl}=0.5$, respectively. The threshold η_w decides which ones in the set α are the most likely newborn target components or clutter-based components after maximum a priori iterations. Generally, the weights of the components originated from clutter are definitely lower than $\eta_w=10^{-3}$. The threshold η_{dl} decides the number of maximum a priori iterations. The smaller value of the threshold η_{dl} will lead to a larger number of iterations and vice versa. The settings of $\eta_w=10^{-3}$ and $\eta_{dl}=0.5$ in our experiments are a proper tradeoff between performance and efficiency.

The mean number of the target estimation error (NTE) [25] and optimal sub-pattern assignment (OSPA) [26] are used to evaluate the performance of different algorithms, where 100 Monte Carlo runs are performed.

$$NTE\ \{X_k,\hat{X}_k\}=E\{|\hat{X}_k|-|X_k|\} \tag{72}$$

$$OSPA_{p,c}\left(X_k,\hat{X}_k\right)=\left(\frac{1}{\left|\hat{X}_k\right|}\min_{\pi\in\Pi_{|\hat{X}_k|}}\sum_{i=1}^{|X_k|}\left(d_c\left(x^i,\hat{x}^{\pi(i)}\right)\right)^p+c^p\times\left(\left|\hat{X}_k\right|-\left|X_k\right|\right)\right)^{1/p} \tag{73}$$

where X_k and $\hat{X}_k$ are the true target set and target estimate set, respectively. The two parameters of the OSPA distance are set to $p=2$ and $c=100$, respectively.

The OSPA distance is a comprehensive metric for evaluating the performance of multiple target tracking algorithms, which reflects the degree of difference between estimation results and true values. Each estimate result consists of the target number and states. $p=2$ and $c=100$ are two classical empirical parameters of the OSPA distance, widely used for multi-target tracking. Generally, the lower OSPA distance, the higher estimation accuracy of target states.

4.2 Experimental Results

As is shown in **Fig. 2**, the true positions of six targets and corresponding measurements are simulated, and the clutter is modeled as a Poisson RFS with the mean $\lambda_c=10\times10^{-6}m^{-2}$. In this scenario, the targets 1 and 2, with the initial states $m_S^1=\left[-700,700,0,0\right]^T$ and $m_S^2=\left[400,850,0,0\right]^T$, respectively, exist during 100 time steps. The other four targets appear and disappear at unknown positions and times.

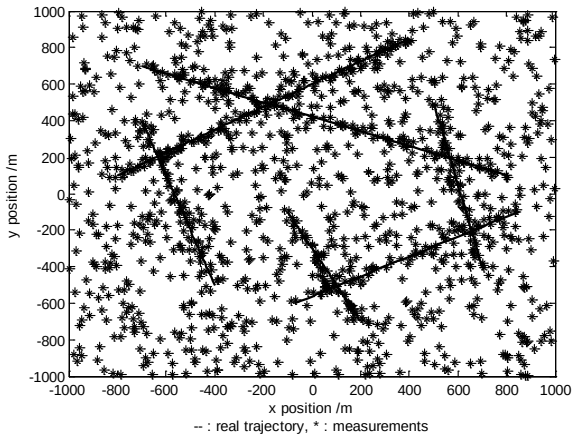

Fig. 2. Trajectories of targets and measurements

Fig. 3 shows the performance comparison in terms of the OSPA distance and NTE for the ABI-GM-PHD filter, extended GM-PHD filter and proposed algorithm. It is clear that the proposed algorithm achieves better performance compared to those of the ABI-GM-PHD and extended GM-PHD filters. However, **Fig. 3(a)** shows that the three algorithms have four high error peaks at the times when newborn targets appear in the tracking scenario. The high error peaks mean that the three algorithms cannot detect newborn targets in time. Usually, one- or two-period lag is needed to estimate newborn targets for the three algorithms. Benefitting from the newborn target intensity estimation and improved measurement-driven schemes, the proposed algorithm achieves a better overall OSPA distance compared to those of the ABI-GM-PHD and extended GM-PHD filters. The NTE of the three algorithms shown in **Fig. 3(b)** also illustrates better performance of the proposed algorithm, where the NTE of the proposed algorithm is relatively low. Better tracking performance in terms of the OSPA distance and NTE obtained by the proposed algorithm demonstrates that the proposed

algorithm can better estimate target states and their number in an environment with unknown positions and times of newborn targets.

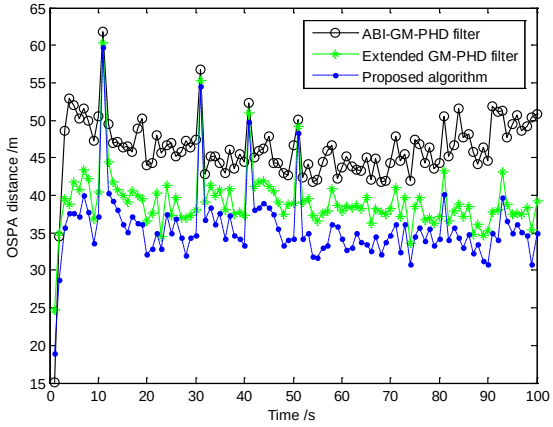

(a) OSPA distance

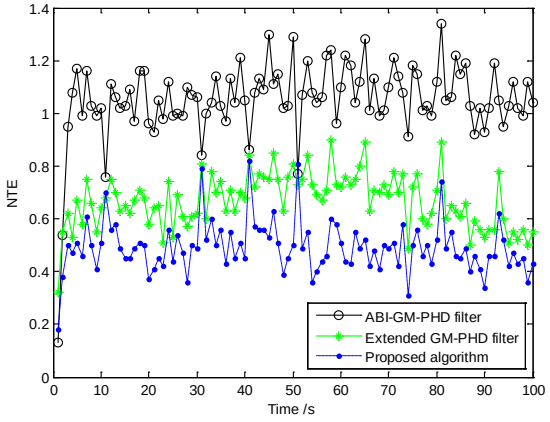

(b) NTE

Fig. 3. OSPA distance and NTE for the three algorithms

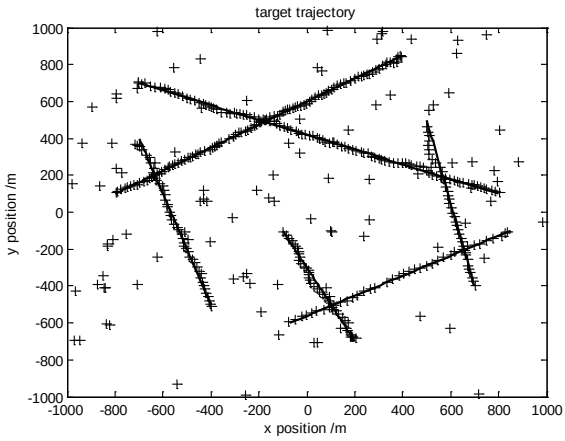

(a) Tracks of the ABI-GM-PHD filter

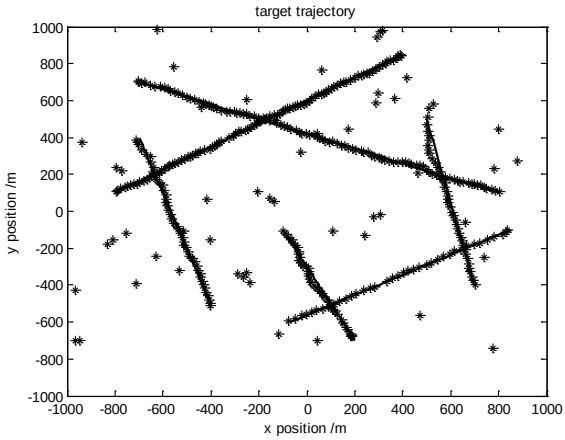

(b) Tracks of the extended GM-PHD filter

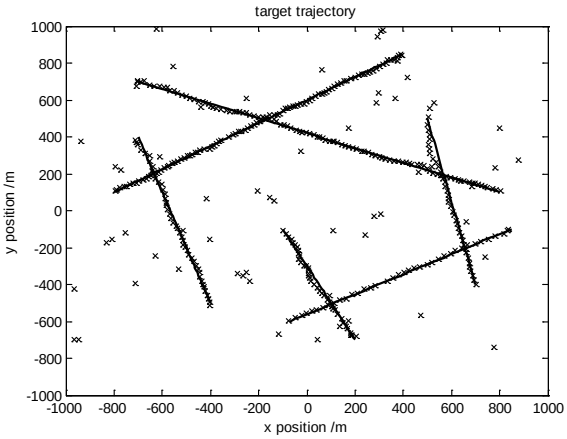

(c) Tracks of the proposed algorithm

Fig. 4. Target tracks of different algorithms

Target position estimates obtained using the proposed algorithm, extended GM-PHD filter and ABI-GM-PHD filter are shown in **Fig. 4**, where the estimated positions are superimposed on the actual tracks over 100 time steps. As evident from **Fig. 4(c)**, the proposed algorithm can detect the tracks of all six targets with few false alarms. In **Fig. 4(a)**, although the ABI-GM-PHD filter can estimate the tracks of all targets, more false alarms are also estimated. In **Fig. 4(b)**, the estimated tracks of the extended GM-PHD filter are similar to those of the proposed algorithm.

Various clutter rates are used to evaluate the performance of the proposed algorithm. The mean number of clutter λ_c changes from 1 to 20, and the detection probability is set to $p_{D,k} = 0.98$. **Table 1** shows the performance comparison among the proposed algorithm, ABI-GM-PHD filter and extended GM-PHD filter. As seen in the table, the effectiveness of the three algorithms decreases when the clutter rate increases. However, the proposed algorithm can achieve good tracking performance in terms of the OSPA distance, NTE, and computational load compared with the ABI-GM-PHD and extended GM-PHD filters. Better performance obtained by the proposed algorithm can be attributed to the newborn target intensity estimation and improved measurement-driven schemes, where accurate target birth intensity can be estimated, and the disturbance of measurements in the update step can be

reduced. Owning to the fact that clutter is removed and forbidden to update targets, the running time obtained by the proposed algorithm keeps increasing slowly even though the clutter rate increases significantly. The lower computational load also makes the proposed algorithm suitable for real-time applications.

Table 1. Comparison of different algorithms under different clutter rates

Mean number of Clutter	1	5	10	15	20
ABI-GM-PHD filter					
OSPA /m	22.36	27.37	37.54	48.86	58.46
NTE	0.059	0.234	0.665	1.321	2.145
Running time /s	1.064	2.176	4.173	7.052	10.89
Extended GM-PHD filter					
OSPA /m	23.10	27.78	36.97	47.22	55.87
NTE	0.073	0.240	0.624	1.193	1.878
Running time /s	0.516	0.895	1.555	2.490	3.688
Proposed algorithm					
OSPA /m	22.69	25.12	32.89	42.61	51.31
NTE	0.092	0.141	0.425	0.881	1.447
Running time /s	0.439	0.656	1.051	1.644	2.401

Table 2 shows simulation results obtained in various detection probability experiments, in which the detection probability is set to $p_{D,k} = 0.8, 0.85, 0.9, 0.95, 1$, and the clutter rate λ_c is kept unchanged at $\lambda_c = 10 \times 10^{-6} m^{-2}$. It is noted that the tracking performance of the ABI-GM-PHD filter, extended GM-PHD filter and proposed algorithm are improved to some extent as the detection probability increases. Clearly, the proposed algorithm achieves lower OSPA distance, the NTE also decreases to the lowest level. Besides, the running time of the proposed algorithm remains at a low level, which is far below that of the ABI-GM-PHD filter. Additionally, the proposed algorithm achieves better performance in terms of the OSPA distance, NTE and running time than the extended GM-PHD filter.

Table 2. Comparison of different algorithms under various detection probabilities

Detection probabilities	0.8	0.85	0.9	0.95	1
ABI-GM-PHD filter					
OSPA /m	66.63	61.79	57.02	50.83	37.81
NTE	1.899	1.690	1.468	1.228	0.672
Running time /s	21.58	18.61	13.91	10.12	4.171
Extended GM-PHD filter					
OSPA /m	55.01	49.78	46.18	41.84	37.30
NTE	0.964	0.840	0.776	0.708	0.635
Running time /s	2.745	2.372	2.087	1.916	1.557
Proposed algorithm					
OSPA /m	53.73	47.99	43.76	38.49	33.07

NTE	0.902	0.759	0.658	0.548	0.429
Running time /s	2.339	1.881	1.564	1.378	1.048

To further assess the performance of the proposed algorithm, various measurement noise experiments are carried out. The values of measurement noises are set to 5, 10, 15, 20 and 25, respectively. **Table 3** shows the comparison results in terms of the OSPA distance, NTE, and running time under various measurement noises. As the measurement noise increases, the efficiency of the ABI-GM-PHD filter, extended GM-PHD filter and proposed algorithm decreases. However, it is clear that both the OSPA distance and NTE of the proposed algorithm are lower than those of the ABI-GM-PHD and extended GM-PHD filters, and speed of the NTE of the proposed algorithm changes more slowly compared to the ABI-GM-PHD and extended GM-PHD filters. Especially, the running time of the proposed algorithm remains almost unchanged, while the running time of the ABI-GM-PHD filter increases significantly.

Table 3. Comparison of different algorithms under different measurement noises

Measurement noises(/m)	5	10	15	20	25
ABI-GM-PHD filter					
OSPA /m	33.39	39.02	46.27	53.61	61.09
NTE	0.493	0.705	1.059	1.519	2.177
Running time /s	7.417	8.062	8.825	9.802	11.04
Extended GM-PHD filter					
OSPA /m	26.86	32.51	39.47	46.32	53.68
NTE	0.257	0.428	0.678	0.982	1.418
Running time /s	1.532	1.678	1.785	1.928	2.143
Proposed algorithm					
OSPA /m	26.03	30.30	35.68	41.33	47.67
NTE	0.232	0.341	0.494	0.680	0.948
Running time /s	1.063	1.161	1.251	1.365	1.540

Remark 2. Being the varieties of the GM-PHD filter, the ABI-GM-PHD filter, extended GM-PHD filter and proposed algorithm have the same computational complexity of the GM-PHD filter, which is $\mathcal{O}(N_k M_k)$, where N_k is the number of targets, and M_k is the number of measurements at time step k.

5. Conclusion

To solve the problem introduced by the unknown newborn target intensity, a dual detection-guided newborn target intensity PHD algorithm is proposed, where the newborn target intensity estimation and improved measurement-driven schemes are introduced. The newborn target intensity estimation scheme composed of the Dirichlet distribution and target velocity feature methods is utilized to obtain the most likely newborn target intensity. Further, an improved measurement-driven scheme is incorporated into the adaptive target birth intensity PHD filter to reduce the errors of the estimated number of targets in dense clutter scenarios, and the computational burden. Simulation results show that the proposed algorithm

is superior to the ABI-GM-PHD and extended GM-PHD filters in terms of the target states, target number and computational load, when the target birth intensity is unknown in multi-target tracking.

References

[1] R. Mahler, Statistical multisource-multitarget information fusion, Artech House, Norwood, MA, pp. 185-195, 2007.

[2] R. Mahler, "Statistics 102 for Multisource-Multitarget Detection and Tracking," *IEEE Journal of Selected Topics in Signal Processing*, vol. 7, no. 3, pp. 376-389, March, 2013. Article (CrossRef Link)

[3] R. Mahler, "PHD filters of higher order in target number," *IEEE Transactions on Aerospace and Electronic Systems*, vol. 43, no. 4, pp. 1523-1543, October, 2007. Article (CrossRef Link)

[4] B.T. Vo, B.N. Vo, A. Cantoni, "The cardinality balanced multi-target multi-Bernoulli filter and its implementations," *IEEE Transactions on Signal Processing*, vol. 57, no. 2, pp. 409-423, October, 2009. Article (CrossRef Link)

[5] B.N. Vo, S. Singh, A. Doucet, "Sequential Monte Carlo implementation of the PHD filter for multi-target tracking," in *Proc. of the 6th International Conference on Information Fusion*, pp. 792-799, 2003. Article (CrossRef Link)

[6] B.N. Vo, W.K. Ma, "The Gaussian mixture probability hypothesis density filter," *IEEE Transactions on Signal Processing*, vol. 54, no. 11, pp. 4091-4104, November, 2006. Article (CrossRef Link)

[7] J. H. Yoon, D. Y. Kim, K. J. Yoon, "Efficient importance sampling function design for sequential Monte Carlo PHD filter," *Signal Processing*, vol. 92, no. 9, pp. 2315-2321, September, 2012. Article (CrossRef Link)

[8] B. Li, F.W. Pang, "Improved probability hypothesis density filter for multitarget tracking," *Nonlinear Dynamics*, vol. 76, no. 1, pp. 367-376, April, 2014. Article (CrossRef Link)

[9] L. Liu, H.B. Ji, Z.H. Fan, "Improved Iterated-corrector PHD with Gaussian mixture implementation," *Signal Processing*, vol. 114, pp. 89-99, September, 2015. Article (CrossRef Link)

[10] S.C. Zhang, J.X. Li, L.B. Wu, "A Novel Multiple Maneuvering Targets Tracking Algorithm with Data Association and Track Management," *International Journal of Control, Automatic, and Systems*, vol. 93, no. 5, pp. 947-956, October, 2013. Article (CrossRef Link)

[11] P. Jan, S. Tomas, N. Zdenek, et.al, "An optimization of a PHD function for association of targets on multistatic radar," in *Proc. of 2014 IEEE Radar Conference*, pp. 1084-1089, 2014. Article (CrossRef Link)

[12] B. Li, "Multiple-model Rao-blackwellized Particle Probability Hypothesis Density Filter for Multitarget Tracking," *International Journal of Control, Automatic, and Systems*, vol. 13, no. 2, pp. 426-433, April, 2015. Article (CrossRef Link)

[13] S. Reuter, B.T. Vo, B.N. Vo, et al., "The Labeled Multi-Bernoulli Filter," *IEEE Transactions on Signal Processing*, vol. 62, no. 12, pp. 3246-3260, May, 2014. Article (CrossRef Link)

[14] B.T. Vo, B.N. Vo, "Labeled Random Finite Sets and Multi-Object Conjugate Priors," *IEEE Transactions on Signal Processing*, vol. 61, no. 13, pp. 3460-3475, April, 2013. Article (CrossRef Link)

[15] B.N. Vo, B.T. Vo, D. Phung, "Labeled Random Finite Sets and the Bayes Multi-Target Tracking Filter," *IEEE Transactions on Signal Processing*, vol. 62, no. 24, pp. 6554-6567, October, 2014. Article (CrossRef Link)

[16] B. Ristic, D. Clark, B.N. Vo, et al., "Adaptive Target Birth Intensity for PHD and CPHD Filters," *IEEE Transactions on Aerospace and Electronic Systems*, vol. 48, no. 2, pp. 1656-1668, April, 2012. Article (CrossRef Link)

[17] Y. Wang, Z.L. Jing, S.Q. Hu, et al., "Detection-guided multi-target Bayesian filter," *Signal Processing*, vol. 92, no. 2, pp. 564-574, February, 2012. Article (CrossRef Link)

[18] H.J. Zhang, J. Wang, B. Ye, et al., "A GM-PHD filter for new appearing targets tracking," in *Proc. of the 6th International Conference on Image and Signal Processing (CISP)*, pp. 1153-1159, 2013. Article (CrossRef Link)
[19] X.L. Zhou, Y.F. Li, B.W. He, et al., "GM-PHD-based multi-target visual tracking using entropy distribution and game theory," *IEEE Transactions on Industrial Informatics*, vol. 10, no. 2, pp. 1064-1076, December, 2014. Article (CrossRef Link)
[20] Y. Q. Zhu, S. L. Zhou, H. X. Zou, et al, "Probability hypothesis density filter with adaptive estimation of target birth intensity," *IET Radar Sonar & Navigation*, Vol. 10, no. 5, pp. 901-911, May, 2016. Article (CrossRef Link)
[21] S. H. Wang, Y. D. Zhang, G. Liu, et al, "Detection of Alzheimer's Disease by Three-Dimensional Displacement Field Estimation in Structural Magnetic Resonance Imaging," *Journal of Alzheimer's Disease*, vol. 50, no. 1, pp. 233-248, October, 2015. Article (CrossRef Link)
[22] Y. D. Zhang, X. J. Yang, C. Cattani, et al, "Tea Category Identification Using a Novel Fractional Fourier Entropy and Jaya Algorithm," *Entropy*, vol. 18, no. 3, pp. 1-17, February, 2016. Article (CrossRef Link)
[23] G. Wu, C.Z. Han, X.X. Yan, "Gaussian mixture implementation of PHD filter based on Dirichlet distribution," in *Proc. of IET International Radar Conference 2013*, pp. 1-6, 2013. Article (CrossRef Link)
[24] M.T. Figueirdo, A.K. Jain, "Unsupervised learning of finite mixture models," *IEEE Transactions on Pattern Analysis and Machine Intelligence*, vol. 24, no. 3, pp. 381-396, March, 2002. Article (CrossRef Link)
[25] M. Yazdian-Dehkordi, Z. Azimifar, M.A. Masnadi-Shirazi, "Competitive Gaussian mixture probability hypothesis density filter for multiple target tracking in the presence of ambiguity and occlusion," *IET Radar, Sonar & Navigation*, vol. 6, no. 4, pp. 251-262, April, 2012. Article (CrossRef Link)
[26] D. Schuhmacher, B.T. Vo, B.N. Vo, "A Consistent Metric for Performance Evaluation of Multi-Object Filters," *IEEE Transactions on Signal Processing*, vol. 56, no. 8, pp. 3447-3457, August, 2008. Article (CrossRef Link)

Li Gao received the M.S degree in computer engineering from Wuhan University, Wuhan, China, in 2010. Since 2010, she has been working as a Lecturer with the Department of Mechanical and Electronic Engineering, Shangqiu Polytechnic. Her research interests include signal processing, and information fusion.

Yongjie Ma received his M.S degree in electronic engineering from Zhengzhou University, Zhengzhou, China, in 1992, Since 2012, he has been working as a Professor with the Department of Mechanical and Electronic Engineering, Shangqiu Polytechnic. His primary areas of research are machinery manufacturing technique and electronic engineering.